Third International Workshop on Radiation of High Temperature Gases in Atmospheric Entry, 2008
TC4-2 - Level 1: Titan atmosphere plasma radiation measurement

M. Playez and D.G. Fletcher

Aeronautic/Aerospace dept., Von Kármán Institute for Fluid Dynamics
1640 Rhode Saint Genèse, Belgium

E-mails: Playez@vki.ac.be, Fletcher@vki.ac.be

Abstract

Emission spectroscopy measurements performed on a plasma representative of Titan atmosphere composition are obtained for temperatures ranging from 3600 to 5000 K, a pressure of 300 mbar and a molar composition of 1.9 % of methane and 98.1 % of nitrogen. The high pressure plasma is produced to obtain conditions close to equilibrium. A good agreement between computed and measured spectra close to the center of the plasma jet is obtained in the spectral range 4300-10000 Å. Similar agreements are obtained for greater radial positions but after application of a correction to account for the fluctuations of the plasma in this region. Optically thin and optically thick reconstructions of the measured intensity spectrum at the center of the jet show strong self-absorption in the spectral range 3500-4300 Å. Comparisons of the measured and computed emissivities and intensities are presented.

Contents

1 Introduction

During aerocapture and entry in the Titan atmosphere, the radiation emitted in the shock layer contributes significantly to the heat flux impinging on the heat shield. Furthermore, most of the radiated energy is emitted in the UV. In this wavelength range, the radiation can penetrate the ablative material comprising the heat shield, heating it in depth and deteriorating its performances. In the considered hypersonic flight conditions, the design of the heat shield requires adequate tools capable of correctly estimating the different heat fluxes. The implementation of equilibrium and non-equilibrium radiation codes necessitates the comparison of the output of the codes and measurements for validation (1)(2). Measurement and modelling of the emission of a plasma representative of Titan atmosphere composition were performed at high pressure in order to validate the equilibrium radiation computation implementation. Results of both the computations and measurements are presented.

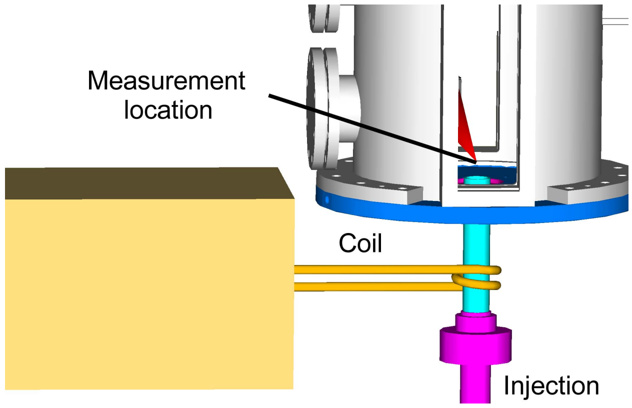

Figure 1: Schematic of the VKI-Minitorch working principle

Table 1: VKI-Minitorch working parameters

Power (in the plasma)	3.75 kW
Frequency	27 MHz
Mixture components	98.1% N_2, 1.9 % CH_4
Mass flow	0.6 g/s
Quartz tube inner diameter	30 mm
Vacuum chamber inner diameter	300 mm
Pressure	300 mbar

2 Definition of the test case

2.1 Facility

The measurements were performed in the VKI-Minitorch facility. The VKI-Minitorch facility is an Inductively Coupled Plasma (ICP) wind tunnel. The working principle of this tunnel is illustrated in figure 1 where a schematic of the wind tunnel is presented. The test gas flows from bottom to top. The mixture of nitrogen and methane enters the quartz tube through the injection block. A Radio Frequency (R.F) current flows in the coil surrounding the quartz tube. It heats the test gas to high temperature through electromagnetic induction. Due to the nature of the heating process, the plasma is, at this location, inherently out of thermal equilibrium. It relaxes toward equilibrium flowing through the quartz tube and the test chamber. The measurements are performed a few centimeters after the end of the quartz tube. The internal pressure of the injection system, quartz tube and test chamber can be continuously varied from 20 mbar to one atmosphere.

2.2 Test conditions

Test conditions for which equilibrium conditions are reached at the measurement location were selected. A plasma at a pressure equal to 300 mbar was investigated. The molar composition of the test gas was 1.9 % of methane and 98.1 % of molecular nitrogen. The different working parameters of the VKI-minitorch are summarized in table 1.

The emission spectroscopy set-up implemented in the VKI-Minitorch facility relied on the measurement of a steady state plasma emission. Nevertheless, during this study, plasma fluctuations were observed. The analysis of those fluctuations are detailed in (4). Optimization of the working conditions of the torch led to a significant decrease of the amplitude of the fluctuations. But the plasma fluctuations could not be fully suppressed. Their possible effects on the emission measurements had to be considered. High speed movies of the plasma jet with acquisition frequencies up to 68 kHz were analyzed. They were obtained using a Phantom v7.0 high speed camera. Spectrally integrated and uncalibrated emission profiles were obtained as

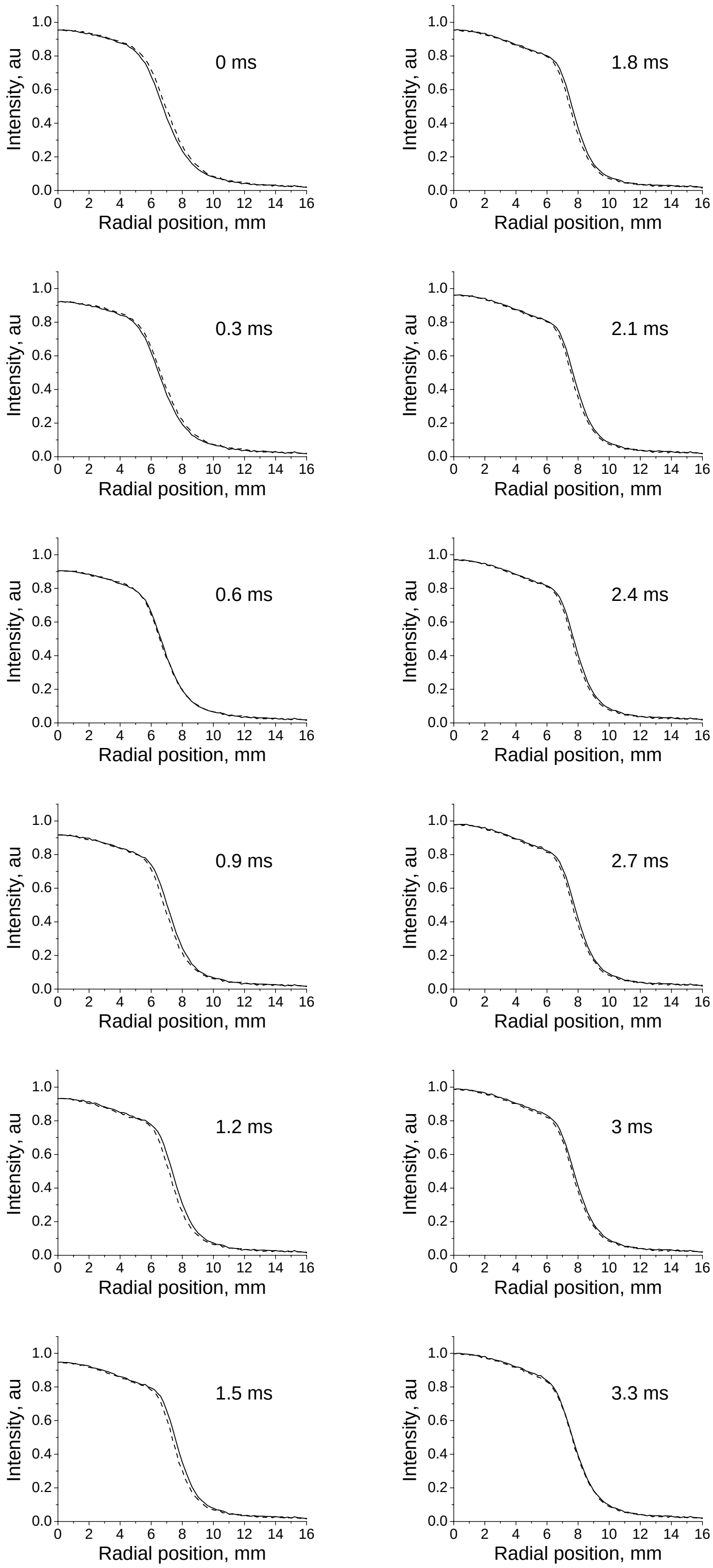

Figure 2: Temporal evolution of the emission profile, Pressure = 300mbar, optimized geometrical configuration

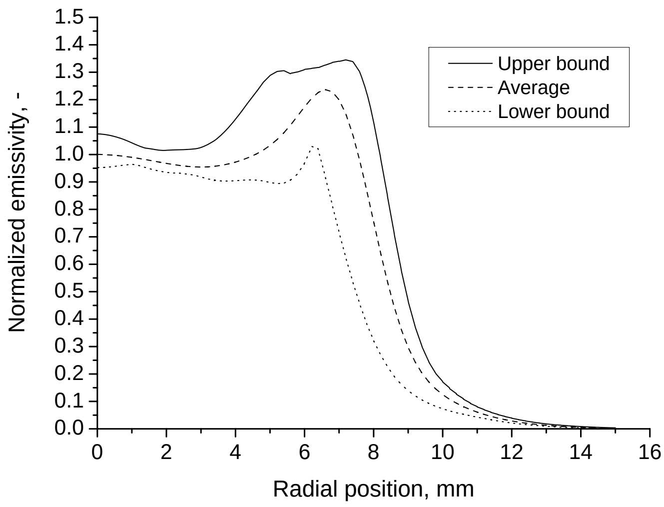

Figure 3: Envelop and average value of the Abel-inverted emission fluctuations in the second configuration, P=300 mbar

	Ocean Optics HR2000-UV-IR
Wavelength range	200 nm - 1100 nm
Grating	300 grooves/mm
F-number	4
Entrance slit width	5 μm
Detector	2048-elements linear silicon CCD array

Table 2: Characteristics of the spectrometer

a function of time. Those profiles are presented in figure 2. The solid line represents the emission profile on one side of the plasma jet (from the center of the jet to the outside of the jet) while the dashed line shows the behavior of the other side. The superposition of the two curves indicates a good symmetry of the plasma flow. The time label printed on each plot indicates the time delay between the acquisition of the picture and the beginning of the sequence. The fluctuations were shown to follow the 300 Hz induction power fluctuations. At 300 mbar no evidence of vortex shedding was observed. In the selected measurement configuration, the amplitude at the center of the jet is small. But large variations occur at the edge of the plasma where large gradients are present. This is illustrated in figure 3 where the envelope and temporal average of the time resolved emission measurements obtained after Abel inversion of the emission profiles are presented.

2.3 Chemical Assumptions

LTE (Local Thermodynamic Equilibrium) conditions are considered. The composition of the plasma was computed using the equilibrium constants of Gurvich (3).

2.4 Radiation Measurements and Computations

2.4.1 Emission spectroscopy measurements

The light emitted by the plasma was collected by a set of UV-enhanced aluminum mirrors before being focused on the entrance of an optical fiber connected to a Ocean Optics HR2000-UV-IR spectrometer. The

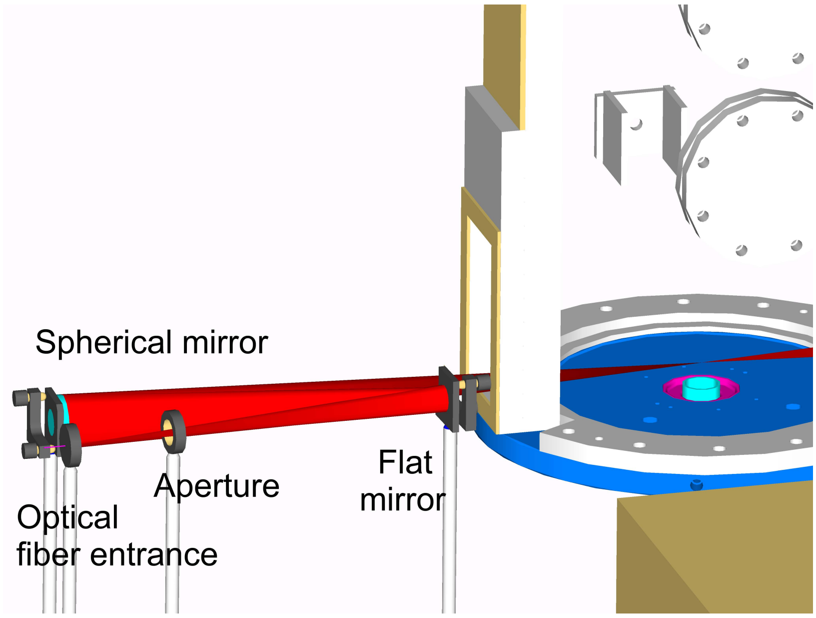

Figure 4: Emission spectroscopic set-up schematic: plasma emission collection optics

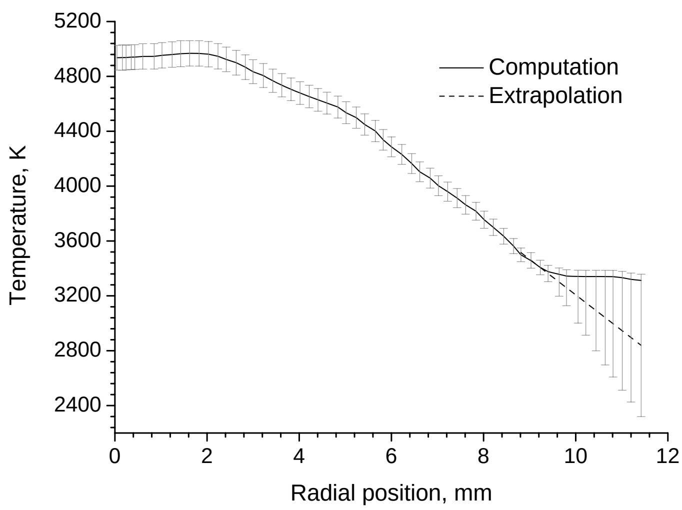

Figure 5: Computed temperature profile

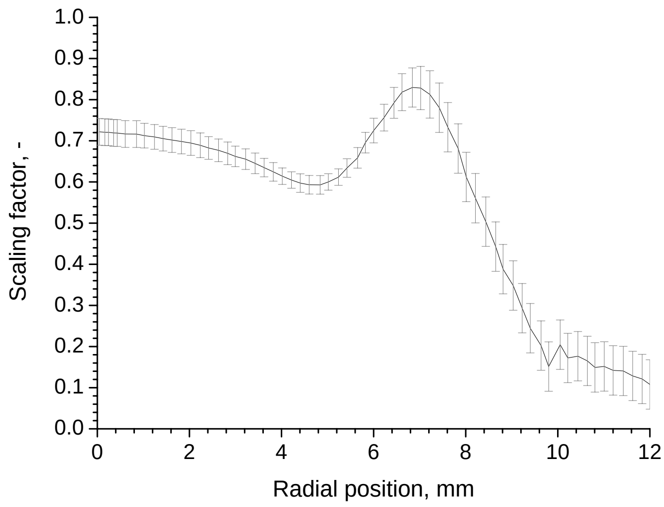

Figure 6: Computed scaling factor profile

characteristics of this spectrometer are summarized in table 2. The details of the optical system are given in figure 4. The light emitted by the plasma flow is collected by a first spherical mirror with a 30 cm focal length. The light is then reflected on a flat mirror before being focused on the entrance of the optical fiber. The magnification of the system is set equal to one. The optical fiber clad plays the role of a field stop. The f-number of the collection optics is kept higher than 25 using an aperture placed in front of the optical fiber. Using this configuration the emission collection volume is a cylinder of diameter close to 320 μm. The whole spectrum from 350 nm to 1000 nm is measured at once. The Full Width at Half Maximum of the apparatus function of the system is equal to 11 Å. The emission measurements were put on a absolute scale using a Tungsten ribbon lamp.

2.4.2 Presentation of the spectra

Synthetic spectra were produced for comparison to the measured spectra. The N_2, CN and C_2 diatomic molecule spectra were considered. The CN Violet, CN Red, CN Leblanc, C_2 Swan, C_2 Phillips, C_2 Deslandres-D'Azambuja and N_2 first and second positive systems were modeled. Only the first four systems show measurable contributions to the total spectrum.
Fitting of the synthetic spectra to the emissivity measurements were performed in the spectral range 4300-9000 Å. In this spectral range, spectral features of the three main systems, CN Violet ($\Delta\nu$=-2), CN red ($\Delta\nu$ ranging from +2 to +6) and C_2 Swan (mainly $\Delta\nu$=-1,0 and +1) are present. The radiation self-absorption is supposed to be negligible and is not taken into account in the computation.
The temperature is adjusted to obtain a good fit on the relative emissivity scale. It is adjusted based on the spectral distribution of the different systems: on the relative strength of the bands and on the distribution in the bands, but also on the relative strength of the different systems of CN and on the relative strength of the systems of two different species CN and C_2. The shape of a band is related to the distribution among the rotational energy levels. The relative strength of the bands is related to the distribution among vibrational energy levels. The relative strength between different systems is related to the distribution among the different electronic energy levels while the relative strength of two systems of two different species includes the distribution among different electronic energy levels but also the composition of the plasma. The fit of the spectra in the considered wavelength interval brings information on the rotational, vibrational and electronic distribution of the energy levels as well as on the composition of the plasma.
If the measurements can be fitted with the LTE (Local Thermodynamic Equilibrium) computation, the previous distributions and the plasma composition can be considered as being close to their equilibrium values. The computed temperature profile is plotted in figure 5.
A global scaling factor, i.e. constant over the whole spectral range, is introduced to obtain a good match on the absolute emissivity scale. The parametrization of the plasma emission by one temperature and a scaling factor was shown to be sufficient to describe properly the emission. The scaling factor, plotted in

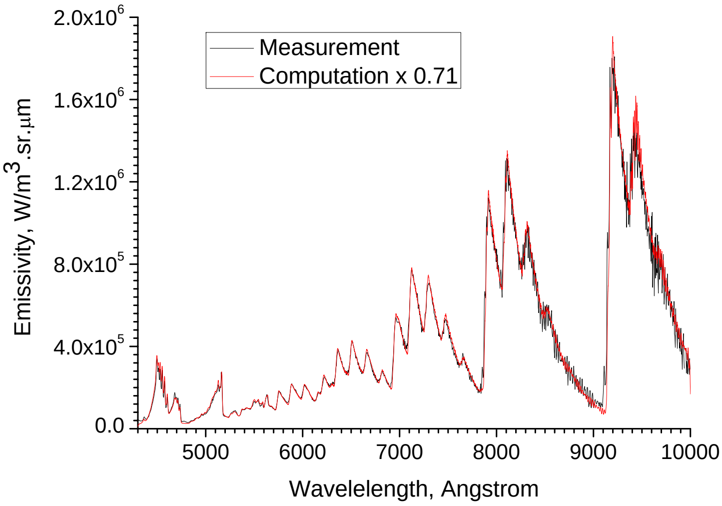

Figure 7: Comparison of the measured and computed emissivities between 4300 and 10000 Å, r=1.24 mm T=4959 K, P=300 mbar, (Computed composition (mole fraction): x_{CN}=4.83×10^{-3}, x_{C_2}=3.40×10^{-5})

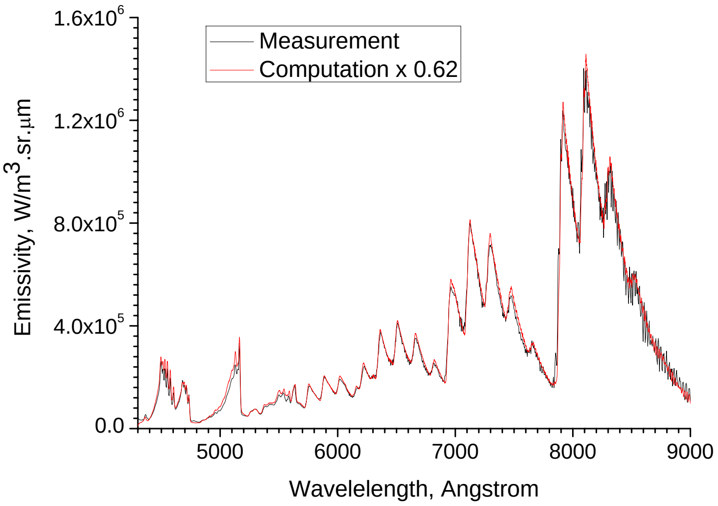

Figure 8: Comparison of the measured and computed emissivities between 4300 and 9000 Å, r=3.82 mm T=4706 K, P=300 mbar, (Computed composition (mole fraction): x_{CN}=6.27×10^{-3}, x_{C_2}=6.07×10^{-5})

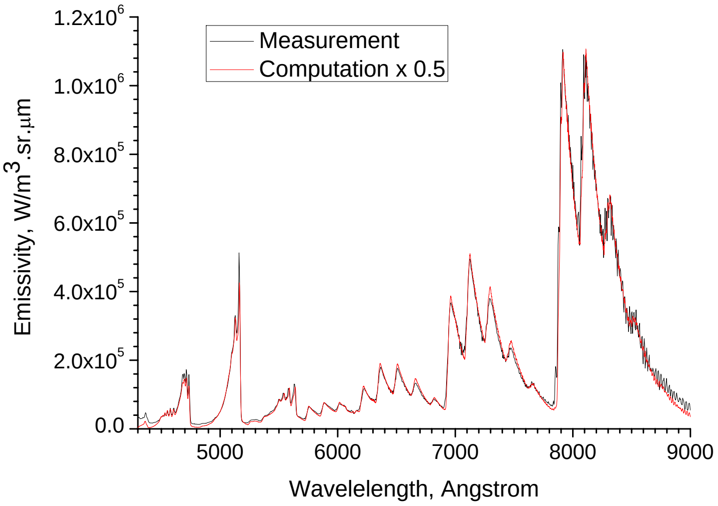

Figure 9: Comparison of the measured and computed emissivities between 4300 and 9000 Å, r=8.43 mm T=3634 K, P=300 mbar, (Computed composition (mole fraction): x_{CN}=1.12×10^{-2}, x_{C_2}=2.88×10^{-4})

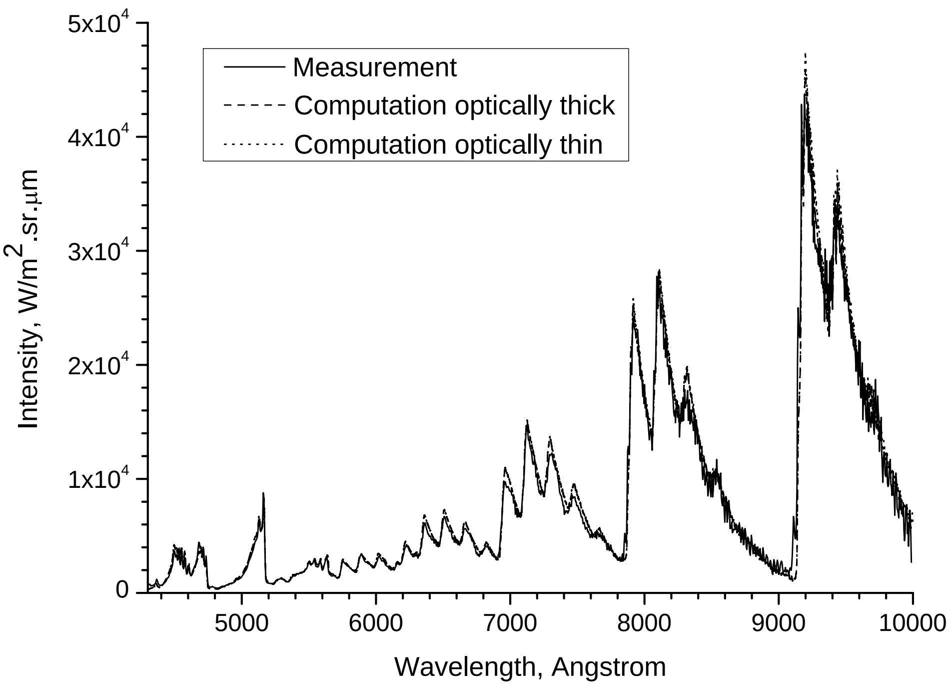

Figure 10: Computed intensity at the center of the jet, 4300-10000 Å interval

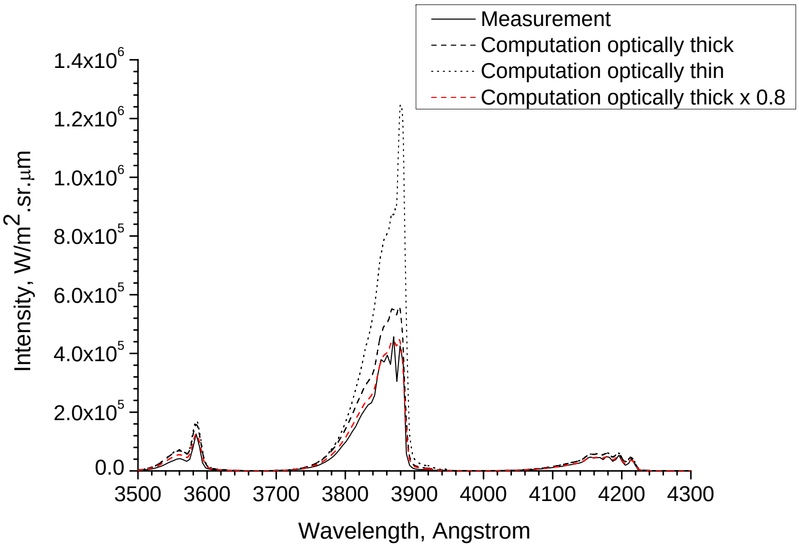

Figure 11: Computed intensity at the center of the jet, 3500-4300 Å interval

figure 6, takes into account the uncertainties of the measurement and modelling but also accounts for the uncertainty in the measurement due to the fluctuations of the plasma (4). While relatively unaffected by the fluctuations at the center of the plasma, the emission has to be corrected by large amounts for radial positions greater than 8 mm. For Radial positions greater than 9 mm, the quality of the fit deteriorates and a linear extrapolation of the temperature profile is preferred to the computed temperature values. The quality of the fit between measurement and model are shown in figures 7, 8 and 9 for three different temperature values ranging from 3600 to 5000 K. The multiplication factor given in the label of the computed spectra is the value of the scaling factor. Estimates of the uncertainty of the computations and measurements, 10 and 21 % at the center of the jet, can reasonably account for the observed discrepancy. At this location the scaling factor equals 0.72 which corresponds to a 28 % error.
Reconstruction of the intensity measured at the center of the jet was performed using the temperature and scaling factor profiles given in figures 5 and 6. The computations was performed solving the radiative transport equation along the plasma diameter corresponding to the optical axis of the emission light collection system. Optically thin and optically thick computations were compared. The results of this computations are plotted in figures 11 and 10. No difference can be made between the optically thin and the optically thick computations in the spectral range 4300-10000 Å, thereby validating the previously made assumption of negligible self-absorption in this range. In the spectral range 3500-4300 Å, strong self-absorption is observed. The CN violet main sequence is attenuated by a factor 2. The optically thick computation reproduce the measurement within 20 %. This last discrepancy can partly be explained by the increase of the calibration uncertainty for lower wavelength and/or a small departure from equilibrium of the highly radiating CN B $^2\Sigma^+$ levels. But the strongest contribution to uncertainty comes from the fluctuations of the plasma. Time resolved measurements would have to be performed first to establish the origin of the observed discrepancy.

3 Input data

The measured spectra of figure 7, 8, 9, 10 and 11 form the data set available for comparison with the output of radiation codes. The emissivity spectra are given in W/m^3.sr.μm and the intensity spectra in W/m^2.sr.μm. The spectra are presented in two-column tables with in the first column the wavelength in Å and in the second column either the emissivity or intensity values. The temperature and pressure values necessary for the computation of the emissivity spectra of figures 7, 8 and 9 are given in the caption of each figure. The names of the files containing the emissivity spectra are Emissivity-r1.24mm.dat, Emissivity-r3.82mm.dat and Emissivity-r8.43mm.dat, where the numbers refer to the different radial positions given in the caption of figures 7, 8 and 9. The intensity spectra are given in files Intensity4300-10000A.dat and Intensity3500-4300A.dat. The temperature and scaling factor profiles are necessary for the computation of the intensity spectra. They are presented in two-column tables with the radial position (in millimeter) in the first column and the temperature (in Kelvin) or scaling factor (without any unit) in the second column. The corresponding file names are TemperatureProfile.dat and ScalingFactorProfile.dat. The mole fraction profiles of CN and C_2 are given in the file CompositionProfile.dat where the first column corresponds to the radial position (in millimeter), the second column to the mole fraction of CN and the third column to the mole fraction of C_2. The apparatus function file has a two-column format, with the wavelength in Å in the first column and the apparatus function in the second column in μm^{-1}. The name of the file is Apparatus.dat.

4 Format of the results

The computed emissivity and intensity spectra will be given in the two-column table format with in the first column the wavelength in Å and in the second column the emissivity in $\text{W/m}^3.\text{sr}.\mu\text{m}$ or the intensity in $\text{W/m}^2.\text{sr}.\mu\text{m}$. The name of the output files correspond to the name of the input files containing the measurements: OutputEmissivity-r1.24mm.dat, OutputEmissivity-r3.82mm.dat, OutputEmissivity-r8.43mm.dat, OutputIntensity4300-10000A.dat and OutputIntensity3500-4300A.dat.

References

[1] Laux C.O., "Optical Diagnostics and Radiative Emission of Air Plasma", HTGL Report No. T-288, Stanford University, Aug. 1993.

[2] Laux C.O., "Physico-chemical models for high enthalpy and plasma flows", Von Karman Institute Lecture Series, 2002.

[3] Gurvich L.V. and Veyts I.E. and Alcock C.B. , "Thermodynamic Properties of Individual Substances. Fourth Edition", Hemisphere publishing Corporation, 1989.

[4] Playez M., "Titan atmosphere plasma investigation using spectroscopic techniques", PhD Thesis, Von Karman Institute - Ecole Centrale Paris, to be published.